

Boundary effects on osmophoresis: Motion of a spherical vesicle perpendicular to two plane walls

Yun S. Hsu, Huan J. Keh*

Department of Chemical Engineering, National Taiwan University, Taipei 10617, Taiwan, ROC

Received 4 March 2005; received in revised form 14 May 2005; accepted 17 July 2005

Available online 31 August 2005

Abstract

The problem of the osmophoretic motion of a spherical vesicle situated at an arbitrary position between two infinite parallel plane walls is studied theoretically in the quasisteady limit of negligible Peclet and Reynolds numbers. The imposed solute concentration gradient is uniform and perpendicular to the plane walls. The presence of the confining walls causes two basic effects on the vesicle velocity: first, the local concentrations on both sides of the vesicle surface are altered by the walls, thereby speeding up or slowing down the vesicle; secondly, the walls enhance the viscous interaction effect on the moving vesicle. To solve the equations of conservation of mass and momentum, the general solutions are constructed from the superposition of the fundamental solutions in both cylindrical and spherical coordinates. The boundary conditions are enforced first at the plane walls by the Hankel transform and then on the vesicle surface by a collocation technique. Numerical results for the osmophoretic velocity of the vesicle relative to that under identical conditions in an unbounded solution are presented for various values of the relevant properties of the vesicle–solution system as well as the relative separation distances between the vesicle and the plane walls. The collocation results agree well with the approximate analytical solutions obtained by using a method of reflections. The presence of the neighboring walls will enhance the vesicle velocity, but its dependence on the relative vesicle–wall separation distances is not necessarily monotonic. The boundary effect on osmophoresis of a vesicle normal to two plane walls is found to be significant and stronger than that parallel to the confining walls.

© 2005 Elsevier Ltd. All rights reserved.

Keywords: Osmophoresis; Colloidal phenomena; Fluid mechanics; Semipermeable vesicle; Plane walls; Boundary effect

1. Introduction

When a vesicle, which is a body of fluid surrounded by a semipermeable membrane, is placed in a solution possessing a solute concentration gradient, one pole of the vesicle sees a higher solute concentration (and hence a higher osmotic pressure) than the opposite pole. The osmotic driving force causes solvent to cross the vesicle's membrane from inside to outside at the high concentration pole, and from outside to inside at the low concentration pole. The vesicle thus functions as a microengine sucking fluid into it on one side and ejecting fluid on the other, thereby advancing toward regions

of low concentration (i.e., in the direction of the solute diffusion current). This phenomenon of vesicle movement is termed osmophoresis (Gordon, 1981; Pope, 1982; Anderson, 1983; Zinemanas and Nir, 1995) and could play some role in the motility of biological vesicles and cells. Applications of osmophoretic motion might also be found in the targeting of encapsulated drugs and other agents toward a microscopic region.

Anderson (1983, 1984) analyzed the osmophoretic motion of a spherical or ellipsoidal vesicle with a thin, rigid membrane in considerable detail. He calculated the drift velocity of the vesicle placed in an unbounded fluid with a prescribed linear solute concentration distribution $C_\infty(\mathbf{x})$ far away from the vesicle for a quite general case. In most physically realistic systems, the velocity \mathbf{U}_0 of a semipermeable spherical vesicle of radius a is linearly related to the uniform

* Corresponding author. Fax: +886 2 23623040.

E-mail address: huan@ntu.edu.tw (H.J. Keh).

concentration gradient ∇C_∞ by the expression

$$\mathbf{U}_0 = -A\nabla C_\infty, \quad (1a)$$

where the vesicle's mobility

$$A = \frac{aL_pRT}{2 + 2\bar{\kappa} + \kappa}, \quad (1b)$$

with dimensionless parameters

$$\kappa = aL_pRT\frac{C_0}{D}, \quad (2a)$$

$$\bar{\kappa} = aL_pRT\frac{\bar{C}}{D}. \quad (2b)$$

In the above equations, L_p is the hydraulic coefficient which is a constant for a given membrane and solvent (equal to the superficial fluid velocity divided by the normal stress difference across the membrane), \bar{D} and D are the solute diffusion coefficients inside and outside the vesicle, respectively, \bar{C} is the average internal concentration of solute, and C_0 denotes the value of C_∞ at the position of the vesicle center. The van't Hoff law (the osmotic pressure Π is linearly related to the solute concentration C by the formula $\Pi = CRT$, where R is the gas constant and T is the absolute temperature) for an ideal solution was used in the derivation of Eq. (1); if Π is not a linear function of C at fixed temperature, then RT must be replaced by $\partial\Pi/\partial C$, evaluated at C_0 in Eqs. (1b) and (2a) and at \bar{C} in Eq. (2b).

Typical values of the parameters in Eq. (1) for biological vesicles in aqueous solutions are $L_p = 10^{-8} \text{ m}^2 \text{ s/kg}^{-1}$, $|\nabla C_\infty| = 10^5 \text{ mol m}^{-4}$, and κ and $\bar{\kappa}$ of order unity (obviously, depending on the concentrations and diffusivities of the solutes and the size of the vesicle). Eq. (1) shows that the vesicle always moves toward regions of lower C_∞ , no matter what the relative values of C_0 and \bar{C} are. Increases in the value of parameter κ or $\bar{\kappa}$ have a retarding effect on the vesicle velocity. A recent experimental work reported that model lipid (dimyristoyl phosphatidylcholine) vesicles of a 10- μm radius in a sucrose or salt concentration gradient of 10^4 mol m^{-4} (the lipid bilayers permit passage of water molecules but not of solute molecules) have a drift velocity of a few micrometers per second (Nardi et al., 1999), which is a little greater than but still close to that predicted by Eq. (1).

Eq. (1) serves only for external fluids that extend to infinity in all directions. In real situations of osmophoresis, however, vesicles are not isolated and will move in the presence of neighboring boundaries. Using a method of reflections, Anderson (1986) obtained analytically the migration velocity of a spherical vesicle undergoing osmophoresis along the axis of a long circular pore with an impermeable wall for the special case of $\kappa = \bar{\kappa} = 0$. His result indicates that the vesicle velocity *increases* monotonically as the ratio of vesicle-to-pore radii increases. This behavior, which is opposite to intuition and occurs because the flow of solvent accompanying the osmophoretic vesicle is opposite to the direction

of vesicle movement, was also observed experimentally by Berg and Turner (1990) for the chemotaxis of *Escherichia coli* and mutants in 10- and 50- μm -diameter capillary tubes. On the other hand, the osmophoretic motion of a spherical vesicle in an arbitrary direction with respect to a plane wall was examined by Keh and Yang (1993a,b) through an exact representation in spherical bipolar coordinates, while the motion parallel to two plane walls at an arbitrary position between them was investigated by Chen and Keh (2003) using a boundary collocation method. Numerical results of wall-correction to Eq. (1) for the vesicle velocity were presented for various values of the relative separation distances and parameters κ and $\bar{\kappa}$. For the general cases considered in these works, the osmophoretic mobility of the vesicle was also found to increase as the vesicle approaches the plane wall.

In this article our purpose is to obtain exact numerical solutions and approximate analytical solutions for the osmophoretic motion of a spherical vesicle perpendicular to two plane walls at an arbitrary position between them. The effects of fluid inertia as well as solute convection are neglected. As will be shown from the method-of-reflection analysis in Appendix A, for the case of a vesicle with $\kappa \ll 1 + \bar{\kappa}$, the solute diffusion around the vesicle undergoing osmophoresis normal to the plane walls will generate smaller concentration gradients along the vesicle surface relative to those in an infinite medium. These concentration gradients reduce the osmophoretic velocity, although it will be enhanced by the viscous interaction between the migrating vesicle and the confining boundaries. Both effects of this solutal retardation and the hydrodynamic enhancement increase as the relative vesicle-wall separation distances decrease. Determining which effect is overriding at small vesicle-wall gap widths is a main target of this study. Because the governing equations and boundary conditions concerning the general problem of osmophoresis of a vesicle at an arbitrary position between two parallel plane walls are linear, its solution can be obtained as a superposition of the solutions for its two subproblems: motion parallel to the plane walls, which was previously examined (Chen and Keh, 2003), and motion normal to the confining walls, which is considered in this article.

2. Analysis

We consider the quasisteady axisymmetric osmophoresis of a spherical vesicle of radius a surrounded by a thin semipermeable membrane in a liquid solution perpendicular to two infinite plane walls whose distances from the center of the vesicle are b and c , as shown in Fig. 1. Here (ρ, ϕ, z) and (r, θ, ϕ) denote the circular cylindrical and spherical coordinate systems, respectively, and the origin of coordinates is chosen at the vesicle center. A linear concentration field $C_\infty(z)$ with a uniform solute gradient $-E_\infty \mathbf{e}_z (= \nabla C_\infty)$ is imposed in the ambient fluid far removed from the vesicle,

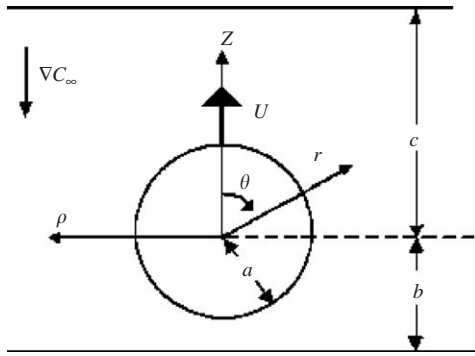


Fig. 1. Geometrical sketch for the osmophoresis of a spherical vesicle perpendicular to two plane walls at an arbitrary position between them.

where \mathbf{e}_z is the unit vector in the z direction and, for convenience, E_∞ is taken to be positive. The vesicle is assumed to maintain its spherical shape and no solute can be transferred across its membrane. The objective is to obtain the correction to Eq. (1) for the vesicle velocity due to the presence of the plane walls.

To determine the osmophoretic velocity of the vesicle, it is necessary to ascertain the solute concentration distributions inside and outside the vesicle and the velocity field in the surrounding fluid phase.

2.1. Solute concentration distribution

For the solute transport in a system of osmophoresis, the Peclet number can be assumed to be small (typical values are $a = 2 \mu\text{m}$ for the vesicle radius, $V = 2.5 \mu\text{m s}^{-1}$ for the characteristic fluid velocity, and $D = 10^{-9} \text{m}^2 \text{s}^{-1}$ for the solute diffusivity; and thus, $Pe = 2aV/D = 0.01$). Hence, the equations of continuity governing the solute concentration distributions for the external and internal fluids are

$$\nabla^2 C = 0 \quad (r \geq a) \quad (3a)$$

and

$$\nabla^2 C_1 = 0 \quad (r \leq a), \quad (3b)$$

respectively. Here, the system is assumed to be isothermal so that the solute diffusion coefficients inside and outside the vesicle are both constant. Because the radius of the vesicle is much greater than the thickness of its membrane, $r = a$ can represent both the inner and outer membrane surfaces of the vesicle.

The concentration distributions are subject to the boundary conditions (Anderson, 1983; Keh and Yang, 1993a)

$$r = a: \frac{\partial C_1}{\partial r} = \frac{\bar{\kappa}}{a} [C - C_0 - (C_1 - \bar{C})], \quad (4a)$$

$$\frac{\partial C}{\partial r} = \frac{\kappa}{a} [C - C_0 - (C_1 - \bar{C})], \quad (4b)$$

where the definitions of the parameters κ and $\bar{\kappa}$ (proportional to C_0 and \bar{C} , respectively) are given by Eq. (2). Since the

solute concentration far away from the vesicle approaches the undisturbed quantities, we can write

$$z = c: C = C_0 - E_\infty c, \quad (5)$$

$$z = -b: C = C_0 + E_\infty b, \quad (6)$$

$$\rho \rightarrow \infty: C \rightarrow C_\infty = C_0 - E_\infty z. \quad (7)$$

The concentrations at the two parallel plane walls have been set equal to different constants to allow a uniform solute gradient in their normal direction far from the vesicle.

The external concentration distribution C , which is governed by the linear Laplace equation, can be expressed as the superposition

$$C = C_0 - E_\infty z + C_w + C_p. \quad (8)$$

Here, C_w is a separable solution of Eq. (3a) in cylindrical coordinates that represents the disturbance produced by the plane walls and is given by a Fourier–Bessel integral

$$C_w = E_\infty \int_0^\infty [X(\omega)e^{\omega z} + Y(\omega)e^{-\omega z}] \omega J_0(\omega \rho) d\omega, \quad (9)$$

where J_n is the Bessel function of the first kind of order n and $X(\omega)$ and $Y(\omega)$ are unknown functions of the separation variable ω . The last term on the right-hand side of Eq. (8), C_p , is a separable solution of Eq. (3a) in spherical coordinates representing the disturbance generated by the vesicle and is given by an infinite series in harmonics,

$$C_p = E_\infty \sum_{m=0}^{\infty} R_m r^{-m-1} P_m(\cos \theta), \quad (10)$$

where P_m is the Legendre polynomial of order m and R_m are unknown constants. Note that a solution for C of the form given by Eqs. (8)–(10) immediately satisfies the boundary condition at infinity in Eq. (7). Since the solute concentration is finite for any position in the interior of the vesicle, the solution to Eq. (3b) can be written as

$$C_1 = \bar{C} - E_\infty z + E_\infty \sum_{m=0}^{\infty} \bar{R}_m r^m P_m(\cos \theta), \quad (11)$$

where \bar{R}_m are unknown constants.

Substituting the concentration distribution C given by Eqs. (8)–(10) into the boundary conditions (5) and (6) and applying the Hankel transform on the variable ρ lead to a solution for the functions $X(\omega)$ and $Y(\omega)$ in terms of the coefficients R_m . After the substitution of this solution into Eqs. (8)–(10), C can be expressed as

$$C = C_0 - E_\infty z + E_\infty \sum_{m=0}^{\infty} R_m \delta_m^{(1)}(r, \theta), \quad (12)$$

where the function $\delta_m^{(1)}(r, \theta)$ is defined by Eq. (B.1) in Appendix B. Applying the boundary conditions given by

Eq. (4) to Eqs. (11) and (12) yields

$$\sum_{m=0}^{\infty} [R_m \bar{\kappa} \delta_m^{(1)}(a, \theta) - \bar{R}_m (\bar{\kappa} + m) a^m P_m(\cos \theta)] = -a \cos \theta, \quad (13a)$$

$$\sum_{m=0}^{\infty} \{R_m [\kappa \delta_m^{(1)}(a, \theta) - a \delta_m^{(2)}(a, \theta)] - \bar{R}_m \kappa a^m P_m(\cos \theta)\} = -a \cos \theta, \quad (13b)$$

where the definition of the function $\delta_m^{(2)}(r, \theta) [= \partial \delta_m^{(1)} / \partial r]$ is given by Eq. (B.2).

To satisfy the conditions in Eq. (13) exactly along the entire surface of the vesicle would require the solution of the entire infinite array of unknown constants R_m and \bar{R}_m . However, the collocation method (O'Brien, 1968; Ganatos et al., 1980; Chen and Keh, 2003) enforces the boundary conditions at a finite number of discrete points on any semi-circular longitudinal generating arc of the sphere (from $\theta=0$ to $\theta=\pi$) and truncates the infinite series in Eqs. (11) and (12) into finite ones. If the spherical boundary is approximated by satisfying the conditions of Eq. (4) at M discrete points on the generating arc, the infinite series in Eqs. (11) and (12) are truncated after M terms, resulting in a system of $2M$ simultaneous linear algebraic equations in the truncated form of Eq. (13). This matrix equation can be numerically solved to yield the $2M$ unknown constants R_m and \bar{R}_m required in the truncated form of Eqs. (11) and (12) for the solute concentration distributions. The accuracy of the boundary-collocation/truncation technique can be improved to any degree by taking a sufficiently large value of M . Naturally, as $M \rightarrow \infty$ the truncation error vanishes and the overall accuracy of the solution depends only on the numerical integration required in evaluating the functions $\delta_m^{(1)}$ and $\delta_m^{(2)}$ in Eq. (13).

2.2. Fluid velocity distribution

Having obtained the solutions for the internal and external solute concentration distributions on the vesicle surface whose difference drives the osmophoretic migration, we can now proceed to find the flow field. Owing to the low Reynolds number encountered in osmophoresis, the fluid motion outside the vesicle is governed by the quasisteady fourth-order differential equation for viscous axisymmetric creeping flows,

$$E^2(E^2\Psi) = 0, \quad (14)$$

in which the Stokes stream function Ψ is related to the velocity components in cylindrical coordinates by

$$v_\rho = \frac{1}{\rho} \frac{\partial \Psi}{\partial z}, \quad (15a)$$

$$v_z = -\frac{1}{\rho} \frac{\partial \Psi}{\partial \rho}, \quad (15b)$$

and the Stokes operator E^2 has the form

$$E^2 = \rho \frac{\partial}{\partial \rho} \left(\frac{1}{\rho} \frac{\partial}{\partial \rho} \right) + \frac{\partial^2}{\partial z^2}. \quad (16)$$

The boundary conditions for the fluid velocity at the vesicle surface (Anderson, 1983; Keh and Yang, 1993a), on the plane walls, and far from the vesicle are

$$r = a: \mathbf{v} = U \mathbf{e}_z + L_p RT [C - C_0 - (C_1 - \bar{C})] \mathbf{e}_r, \quad (17)$$

$$z = c, -b: \mathbf{v} = \mathbf{0}, \quad (18)$$

$$\rho \rightarrow \infty: \mathbf{v} = \mathbf{0}. \quad (19)$$

Here, \mathbf{e}_r is the unit vector in the r direction and U is the osmophoretic velocity of the vesicle to be determined.

To solve the flow field, we express the stream function in the form (Ganatos et al., 1980)

$$\Psi = \Psi_w + \Psi_p. \quad (20)$$

Here Ψ_w is a Fourier–Bessel integral solution of Eq. (14) in cylindrical coordinates that represents the disturbance produced by the plane walls and is given by

$$\Psi_w = \int_0^\infty [A(\omega)e^{\omega z} + B(\omega)e^{-\omega z} + C(\omega)\omega z e^{\omega z} + D(\omega)\omega z e^{-\omega z}] \rho J_1(\omega \rho) d\omega, \quad (21)$$

where $A(\omega)$, $B(\omega)$, $C(\omega)$, and $D(\omega)$ are unknown functions of ω . The second part of Ψ , denoted by Ψ_p , is a solution of Eq. (14) in spherical coordinates representing the disturbance generated by the sphere and is given by

$$\Psi_p = \sum_{n=2}^{\infty} (B_n r^{-n+1} + D_n r^{-n+3}) G_n^{-1/2}(\cos \theta), \quad (22)$$

where $G_n^{-1/2}$ is the Gegenbauer polynomial of the first kind of order n and degree $-1/2$; B_n and D_n are unknown constants. Note that the boundary condition in Eq. (19) is immediately satisfied by a solution of the form given by Eqs. (20)–(22).

Substituting the stream function Ψ given by Eqs. (20)–(22) into the boundary conditions in Eq. (18) and applying the Hankel transform on the variable ρ lead to a solution for $A(\omega)$, $B(\omega)$, $C(\omega)$, and $D(\omega)$ in terms of the coefficients B_n and D_n . After the substitution of this solution into Eqs. (20)–(22), the fluid velocity components can be expressed as

$$v_\rho = \sum_{n=2}^{\infty} [B_n \gamma_{1n}^{(1)}(r, \theta) + D_n \gamma_{2n}^{(1)}(r, \theta)], \quad (23a)$$

$$v_z = \sum_{n=2}^{\infty} [B_n \gamma_{1n}^{(2)}(r, \theta) + D_n \gamma_{2n}^{(2)}(r, \theta)], \quad (23b)$$

where the definitions of the functions $\gamma_{in}^{(j)}$ for i and j equal to 1 or 2 (which must be performed numerically) are given by Eqs. (B.5)–(B.8).

The only boundary condition that remains to be satisfied is that on the vesicle surface. Substituting Eqs. (11), (12) and (23) into Eq. (17), one obtains

$$\begin{aligned} & \sum_{n=2}^{\infty} [B_n \gamma_{1n}^{(1)}(a, \theta) + D_n \gamma_{2n}^{(1)}(a, \theta)] \\ &= L_p RTE_{\infty} \sum_{m=0}^{\infty} [R_m \delta_m^{(1)}(a, \theta) \\ & \quad - \bar{R}_m a^m P_m(\cos \theta)] \sin \theta, \end{aligned} \quad (24a)$$

$$\begin{aligned} & \sum_{n=2}^{\infty} [B_n \gamma_{1n}^{(2)}(a, \theta) + D_n \gamma_{2n}^{(2)}(a, \theta)] \\ &= U + L_p RTE_{\infty} \sum_{m=0}^{\infty} [R_m \delta_m^{(1)}(a, \theta) \\ & \quad - \bar{R}_m a^m P_m(\cos \theta)] \cos \theta, \end{aligned} \quad (24b)$$

where the first $2M$ coefficients R_m and \bar{R}_m have been determined through the procedure given in the previous subsection.

Eq. (24) can be satisfied by utilizing the collocation technique presented for the solution of the solute concentration field. At the vesicle surface, Eq. (24) is applied at N discrete points (values of θ between 0 and π) and the infinite series in Eq. (23) are truncated after N terms. This generates a set of $2N$ linear algebraic equations for the $2N$ unknown coefficients B_n and D_n . The fluid velocity field outside the vesicle is completely obtained once these coefficients are solved for a sufficiently large number of N .

2.3. Derivation of the vesicle velocity

The hydrodynamic force acting on the spherical vesicle can be determined from (Happel and Brenner, 1983)

$$F = 4\pi\eta D_2, \quad (25)$$

where η is the fluid viscosity. This expression shows that only the lowest-order coefficient D_2 contributes to the drag force exerted on the vesicle by the external fluid.

Since the vesicle is freely suspended in the surrounding fluid, the net force acting on the vesicle must vanish. Applying this constraint to Eq. (25), one has

$$D_2 = 0. \quad (26)$$

To determine the osmophoretic velocity U of the vesicle, Eq. (26) and the $2N$ algebraic equations resulting from Eq. (24) are to be solved simultaneously.

If the vesicle velocity in Eq. (17) is disabled (i.e., $U = 0$ is set), then the force obtained from Eq. (25) can be taken as the osmophoretic force exerted on the vesicle near the walls due to the solute concentration gradient ∇C_{∞} . This force can be expressed as

$$F = 6\pi\eta a U_0 F^*, \quad (27)$$

where U_0 is a characteristic velocity (the osmophoretic velocity of the vesicle in the absence of the plane walls) given by Eq. (1) and F^* is the normalized magnitude of the osmophoretic force. The value of F^* also equals f^*U/U_0 , where f^* is the dimensionless Stokes resistance coefficient of the vesicle migrating normal to the two plane walls driven by a body force in the absence of the concentration gradient and U is the osmophoretic velocity of the vesicle obtained from Eq. (26).

The dimensionless resistance coefficient f^* of the vesicle is the same as that of an impermeable solid sphere of identical radius translating perpendicular to the two plane walls under a body force field (Ganatos et al., 1980). To see this, the osmophoresis problem can be decomposed into two subproblems: (i) the vesicle at rest under a solute concentration gradient experiences a force that is exactly F given by Eq. (27), and (ii) the vesicle moving at velocity U due to a body force experiences a drag force $6\pi\eta a U f^*$, which is also equal to F such that the net force vanishes. Such an analysis clearly dictates that f^* stands for the resistance coefficient of the vesicle, not really an impermeable sphere. However, in the absence of a concentration gradient, no radial fluid velocity relative to the vesicle center exists at the vesicle surface as seen from Eq. (17), despite a nonzero L_p . This would imply that the drag force on a vesicle under a body force field is equal to that on an impermeable sphere, and solvent permeation across the membrane takes place only in the presence of a concentration gradient.

3. Results and discussion

The numerical results for the osmophoretic motion of a spherical vesicle perpendicular to two plane walls at an arbitrary position between them, obtained by using the boundary collocation method described in the previous section, is presented in this section. The system of linear algebraic equations to be solved for the coefficients R_m and \bar{R}_m is constructed from Eq. (13), while that for B_n and D_n is composed of Eq. (24). All the numerical integrations to evaluate the functions $\delta_m^{(j)}$ and $\gamma_{in}^{(j)}$ were done by the 180-point Gauss–Laguerre quadrature.

When selecting the points along the half-circular longitudinal generating arc of the spherical vesicle where the boundary conditions are to be exactly satisfied, the first points that should be chosen are $\theta = 0$ and $\theta = \pi$, since these points control the gaps between the vesicle and the plane walls. In addition, the point $\theta = \pi/2$ which defines the projected area of the vesicle normal to the direction of motion is also important. However, an examination of the systems of linear algebraic equations in Eqs. (13) and (24) shows that the matrix equations become singular if these points are used. To overcome this difficulty, these three points are replaced by four closely adjacent basic points, i.e., $\theta = \delta$, $\pi/2 - \delta$, $\pi/2 + \delta$, and $\pi - \delta$ (Ganatos et al., 1980). Additional points along the generating arc are selected as mirror-image pairs

Table 1

Numerical results of the normalized osmophoretic force F^* on a spherical vesicle near a plane wall ($c \rightarrow \infty$) caused by a normal solute concentration gradient for the case of $\kappa = \bar{\kappa} = 0$

| a/b | F^* | | |
|-------|---------------|---------------|---------------|
| | $N = M = 104$ | $N = M = 106$ | $N = M = 108$ |
| 0.1 | 1.12717 | 1.12717 | 1.12717 |
| 0.2 | 1.29394 | 1.29394 | 1.29394 |
| 0.3 | 1.52262 | 1.52262 | 1.52262 |
| 0.4 | 1.85106 | 1.85106 | 1.85106 |
| 0.5 | 2.34856 | 2.34856 | 2.34856 |
| 0.6 | 3.15613 | 3.15613 | 3.15613 |
| 0.7 | 4.60887 | 4.60887 | 4.60887 |
| 0.8 | 7.73231 | 7.73231 | 7.73231 |
| 0.9 | 17.7083 | 17.7083 | 17.7083 |
| 0.95 | 38.8115 | 38.8115 | 38.8115 |
| 0.99 | 212.874 | 212.874 | 212.874 |
| 0.995 | 432.54 | 432.55 | 432.55 |
| 0.999 | 2125 | 2133 | 2140 |

about the plane $\theta = \pi/2$ to divide the two quarter-circular arcs of the vesicle into equal segments. The optimum value of δ in this work is found to be 0.1° , with which the numerical results of the vesicle velocity converge satisfactorily.

3.1. Motion normal to a single plane wall

Numerical solutions for the normalized osmophoretic force F^* acting on a spherical vesicle near a single plane wall (with $c \rightarrow \infty$) caused by a normal solute concentration gradient, defined by Eq. (27), for the case of $\kappa = \bar{\kappa} = 0$ are given in Table 1 for various values of the spacing parameter a/b at the quasisteady state using the boundary collocation method. All of these results were obtained by choosing the number of collocation points $N (=M)$ equal to 104, 106, and 108 to show their convergence. The rate of convergence is rapid for small values of a/b and deteriorates monotonically as the distance between the vesicle and the wall decreases. Opposite to intuition, but consistent with the previous solutions obtained for the boundary effects on osmophoresis, the results in Table 1 illustrate that the osmophoretic force exerted on the vesicle increases monotonically and dramatically as the parameter a/b increases. This occurs because the fluid flow accompanying the osmophoretic vesicle is opposite to the direction of its migration.

In Table 2, the collocation solutions for the osmophoretic velocity of a spherical vesicle normal to a plane wall for different values of the parameters κ , $\bar{\kappa}$, and a/b are presented. The velocity for the osmophoretic motion of an identical vesicle in an infinite fluid, U_0 , given by Eq. (1), is used to normalize the wall-corrected quantities. All of the results obtained under the collocation scheme converge satisfactorily to at least the significant figures shown in the table. Again, the accuracy and convergence behavior of the truncation technique is principally a function of the ratio a/b . For the most difficult case with $a/b = 0.999$, the numbers of col-

location points $M = 108$ and $N = 108$ are sufficiently large to achieve this convergence. Through the use of spherical bipolar coordinates, Keh and Yang (1993a) obtained numerical solutions for the normalized osmophoretic velocity of a spherical vesicle perpendicular to a plane wall. These solutions for the case of $\kappa = \bar{\kappa} = 0$ are also presented in Table 2 for comparison. It can be seen that our collocation solutions for the vesicle velocity agree excellently with the bipolar-coordinate solutions. Note that the dimensionless Stokes resistance coefficient $f^* = F^*/(U/U_0)$ for the translation of a sphere normal to a plane wall as a function of a/b can be calculated using the collocation solutions presented in Tables 1 and 2 for the case of $\kappa = \bar{\kappa} = 0$, and the results agree well with those available in the literature (Brenner, 1961; Maude, 1961).

In Appendix A, an approximate analytical solution for the same osmophoretic motion as that considered here is also obtained by using a method of reflections. The vesicle velocity is given by Eq. (A.11), which is a power series expansion in $\lambda (=a/b)$. The values of the wall-corrected normalized vesicle velocity calculated from this asymptotic solution, with the $O(\lambda^9)$ term neglected, are also listed in Table 2 for comparison. It can be seen that the asymptotic formula of Eq. (A.11) from the method of reflections for U/U_0 agrees very well with the exact results as long as $\lambda \leq 0.7$; the errors in all cases are less than 2.2%. However, the accuracy of Eq. (A.11) deteriorates rapidly, as expected, when the relative spacing between the vesicle and the plane wall becomes small. The formula of Eq. (A.11) may overestimate or underestimate the osmophoretic velocity of the vesicle, depending on the combination of the parameters κ , $\bar{\kappa}$, and a/b .

The collocation solutions for the normalized velocity U/U_0 of a spherical vesicle undergoing osmophoresis normal to a plane wall as a function of a/b are depicted in Fig. 2 for various values of κ and $\bar{\kappa}$. As expected, the vesicle drifts with the velocity that would exist in the absence of the wall as $a/b \rightarrow 0$. However, the boundary effect of the plane wall on osmophoretic motion can be quite significant when a/b becomes greater. For instance, the osmophoretic velocity for the case of $\kappa = 10$, $\bar{\kappa} = 0$, and $a/b = 0.95$ can be more than four times as high as the magnitude with the boundary being far away from the vesicle. The wall-corrected normalized osmophoretic mobility U/U_0 of the vesicle increases with an increase in κ and decreases with an increase in $\bar{\kappa}$, keeping each other parameter unchanged. This decrease or increase in the vesicle mobility becomes more pronounced as a/b increases. This behavior is expected knowing that the solute concentration gradients along the vesicle surface near a plane wall increase as the ratio $\kappa/(1 + \bar{\kappa})$ increases (see the analysis in Appendix A). When $\kappa = 1 + \bar{\kappa}$, the effect of solutal interaction between the vesicle and the wall disappears, and the relative osmophoretic mobility of the vesicle is independent of the value of either κ or $\bar{\kappa}$ and increases monotonically with a/b solely owing to the hydrodynamic enhancement exerted by the plane wall.

Table 2

Normalized osmophoretic velocity of a spherical vesicle normal to an infinite plane wall (with $c \rightarrow \infty$) computed from the exact boundary-collocation solution and the asymptotic method-of-reflection solution

| a/b | U/U_0 | | | | | |
|-------|-----------------------------|---------------------|---------------------------------|---------------------|---------------------------------|---------------------|
| | $\kappa = \bar{\kappa} = 0$ | | $\kappa = 10, \bar{\kappa} = 0$ | | $\kappa = 0, \bar{\kappa} = 10$ | |
| | Exact solution ^a | Asymptotic solution | Exact solution | Asymptotic solution | Exact solution | Asymptotic solution |
| 0.1 | 1.00087 (1.0009) | 1.00087 | 1.00118 | 1.00118 | 1.00087 | 1.00087 |
| 0.2 | 1.00689 (1.0069) | 1.00689 | 1.00944 | 1.00944 | 1.00688 | 1.00689 |
| 0.3 | 1.02297 (1.0230) | 1.02301 | 1.03192 | 1.03194 | 1.02290 | 1.02294 |
| 0.4 | 1.05393 (1.0539) | 1.05426 | 1.07690 | 1.07698 | 1.05347 | 1.05387 |
| 0.5 | 1.10493 (1.1049) | 1.10663 | 1.15599 | 1.15579 | 1.10300 | 1.10513 |
| 0.6 | 1.18228 (1.1823) | 1.18849 | 1.28905 | 1.28518 | 1.17567 | 1.18407 |
| 0.7 | 1.29485 (1.2948) | 1.31262 | 1.51652 | 1.49055 | 1.27476 | 1.30160 |
| 0.8 | 1.45746 (1.4575) | 1.49863 | 1.93913 | 1.80893 | 1.39960 | 1.47439 |
| 0.9 | 1.70301 (1.7030) | 1.77600 | 2.91136 | 2.29170 | 1.53337 | 1.72761 |
| 0.95 | 1.88623 (1.8862) | | 4.10127 | | 1.57949 | |
| 0.99 | 2.10988 (2.1099) | | 6.70229 | | 1.56039 | |
| 0.995 | 2.15171 (2.1517) | | 7.5492 | | 1.54561 | |
| 0.999 | 2.1934 | | 8.39 | | 1.5258 | |

^aValues in parentheses were obtained by Keh and Yang (1993a) using bipolar coordinates.

Examination of the results shown in Table 2 and Fig. 2 reveals an interesting feature. For the case $\kappa \ll 1 + \bar{\kappa}$, the osmophoretic mobility of a vesicle in the direction normal to a plane wall increases with an increase in a/b as a/b is small, but decreases from a maximum with increasing a/b as a/b is sufficiently large. This feature that U/U_0 may not be a monotonic function of a/b is understandable because the wall effect of hydrodynamic enhancement on the vesicle is in competition with the wall effect of solutal retardation when a vesicle with a small value of $\kappa/(1 + \bar{\kappa})$ is undergoing osmophoretic motion normal to a plane wall. Under the situations of a moderate to large value of $\kappa/1 + \bar{\kappa}$, the osmophoretic mobility of the vesicle near the plane wall is a monotonic increasing function of a/b . By the linearity of the problem, the magnitude of the osmophoretic velocity or force is independent of whether the vesicle drifts toward or away from the plane wall.

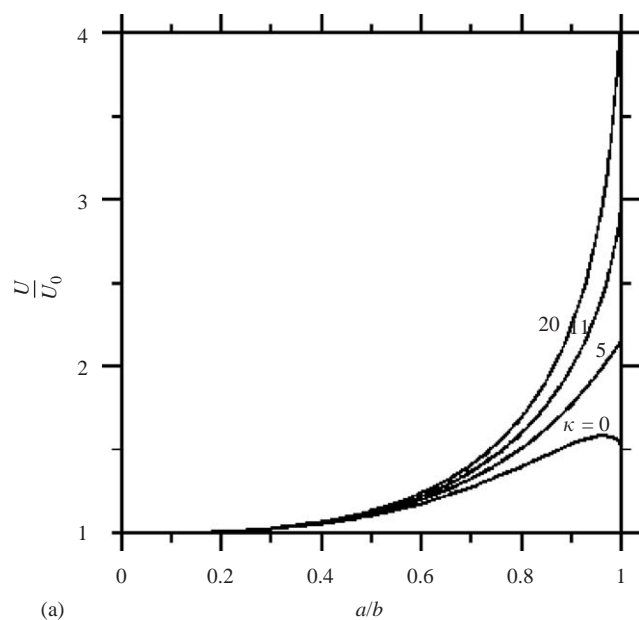
Because the governing equations and boundary conditions concerning the general problem of osmophoresis of a vesicle in an arbitrary direction near a plane wall are linear, the net solution can be obtained as a superposition of the solutions for its two subproblems: motion perpendicular to the plane, which is examined in this paper, and motion parallel to the plane. The collocation solutions for the osmophoretic motion of a spherical vesicle parallel to a plane wall have already been obtained by Chen and Keh (2003). It was found that, when the wall is prescribed with a linear concentration profile consistent with the far-field solute distribution, the wall-corrected normalized osmophoretic velocity of the vesicle also increases with an increase in the ratio $\kappa/(1 + \bar{\kappa})$. A comparison between the Table 3 of Chen and Keh and our Table 2 indicates that the plane wall exerts the most influence on the vesicle when osmophoretic motion occurs nor-

mal to it, and the least in the case of osmophoresis parallel to it. Therefore, the direction of motion of a vesicle near a plane wall is different from that of the solute concentration gradient, except when it is oriented parallel or perpendicular to the plane wall.

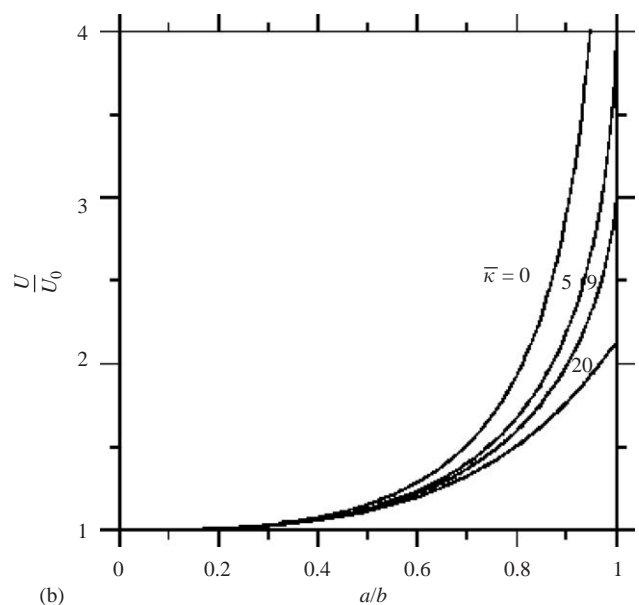
3.2. Motion perpendicular to two plane walls

Numerical results of the normalized osmophoretic force F^* exerted on a spherical vesicle located between two parallel plane walls whose distance to one wall is the same (with $c = b$) or three times as great (with $c = 3b$) as to the other wall caused by a perpendicular solute concentration gradient are presented in Table 3 for various values of the parameter a/b using the boundary-collocation method for the case of $\kappa = \bar{\kappa} = 0$. Similar to the results for a single plane wall given in Table 1, the results in Table 3 were obtained by choosing the number of collocation points $N (=M)$ equal to 104, 106, and 108 to show their convergence. Again, these results indicate that the osmophoretic force acting on the vesicle is a monotonic increasing function of a/b .

In Table 4, the collocation solutions for the normalized velocity U/U_0 of a spherical vesicle situated midway between two parallel plane walls (with $c = b$) or at the position $c = 3b$ undergoing osmophoresis perpendicularly for various values of the parameters κ , $\bar{\kappa}$, and a/b are presented. The corresponding method-of-reflection solutions, given by Eq. (A.20) in Appendix A as a power series expansion in $\lambda (=a/b)$ correct to $O(\lambda^8)$, are also listed in this table for comparison. Similar to the case of migration of a spherical vesicle normal to a single plane wall considered in the previous subsection, the approximate analytical formula of



(a)



(b)

Fig. 2. Plots of the normalized osmophoretic velocity U/U_0 of a spherical vesicle perpendicular to a plane wall versus the separation parameter a/b : (a) for several values of κ with $\bar{\kappa} = 10$; (b) for several values of $\bar{\kappa}$ with $\kappa = 10$.

Eq. (A.20) agrees quite well with the exact results as long as $\lambda \leq 0.6$, but can have significant errors when $\lambda \geq 0.7$. In general, Eq. (A.20) underestimates the osmophoretic velocity of the vesicle. A comparison between Table 4 for the case of a slit and Table 2 for the case of a single normal plane indicates that the assumption that the boundary effect for two walls can be obtained by the simple addition of single-wall effects leads to a greater correction to osmophoretic motion. Analogous to the motion normal to a single plane wall, the dimensionless Stokes resistance coefficient $f^* = F^*/(U/U_0)$ for the translation of a sphere perpendicular to two plane

Table 3

Numerical results of the normalized osmophoretic force F^* on a spherical vesicle located between two parallel plane walls caused by a normal solute concentration gradient for the case of $\kappa = \bar{\kappa} = 0$

| a/b | F^* | | |
|----------|---------------|---------------|---------------|
| | $N = M = 104$ | $N = M = 106$ | $N = M = 108$ |
| $c = b$ | | | |
| 0.1 | 1.17021 | 1.17021 | 1.17021 |
| 0.2 | 1.41076 | 1.41076 | 1.41076 |
| 0.3 | 1.76519 | 1.76519 | 1.76519 |
| 0.4 | 2.30574 | 2.30574 | 2.30574 |
| 0.5 | 3.16174 | 3.16174 | 3.16174 |
| 0.6 | 4.59231 | 4.59231 | 4.59231 |
| 0.7 | 7.20777 | 7.20777 | 7.20777 |
| 0.8 | 12.8693 | 12.8693 | 12.8693 |
| 0.9 | 31.0998 | 31.0998 | 31.0998 |
| 0.95 | 69.3330 | 69.3330 | 69.3330 |
| 0.99 | 384.999 | 384.999 | 384.999 |
| 0.995 | 782.32 | 782.33 | 782.33 |
| 0.999 | 3848 | 3862 | 3875 |
| $c = 3b$ | | | |
| 0.1 | 1.12909 | 1.12909 | 1.12909 |
| 0.2 | 1.29876 | 1.29876 | 1.29876 |
| 0.3 | 1.53168 | 1.53168 | 1.53168 |
| 0.4 | 1.86602 | 1.86602 | 1.86602 |
| 0.5 | 2.37124 | 2.37124 | 2.37124 |
| 0.6 | 3.18801 | 3.18801 | 3.18801 |
| 0.7 | 4.64941 | 4.64941 | 4.64941 |
| 0.8 | 7.77275 | 7.77275 | 7.77275 |
| 0.9 | 17.7643 | 17.7643 | 17.7643 |
| 0.95 | 38.6205 | 38.6205 | 38.6205 |
| 0.99 | 211.061 | 211.061 | 211.061 |
| 0.995 | 428.65 | 428.66 | 428.66 |
| 0.999 | 2105 | 2113 | 2120 |

walls with $c = b$ or $c = 3b$ as a function of a/b can be calculated using the collocation solutions presented in Tables 3 and 4 for the case of $\kappa = \bar{\kappa} = 0$, and the results agree well with those available in the literature (Ganatos et al., 1980).

The collocation results for the normalized osmophoretic mobility U/U_0 of a spherical vesicle on the median plane between two parallel plane walls in the normal direction are plotted in Fig. 3 as a function of a/b for several values of κ and $\bar{\kappa}$. Analogous to the corresponding motion of a vesicle normal to a single plane wall, for a specified value of a/b , U/U_0 increases with an increase in κ and decreases with an increase in $\bar{\kappa}$. Again, for the case of $\kappa \ll 1 + \bar{\kappa}$, the osmophoretic mobility of the vesicle first goes through a maximum with the increase of a/b from $a/b = 0$ and then decreases. For other cases, U/U_0 increases monotonically with an increase in a/b .

A careful comparison of the curves in Fig. 3 for the case of a slit with the corresponding curves in Fig. 2 for the case of a single wall reveals an interesting feature of the boundary effect on osmophoresis of a spherical vesicle. The presence of a second normal plane wall, even at a symmetric position with respect to the vesicle against the first, does

Table 4

Normalized osmophoretic velocity of a spherical vesicle normal to two parallel plane walls computed from the exact boundary-collocation solution and the asymptotic method-of-reflection solution

| a/b | U/U_0 | | | | | |
|----------|-----------------------------|---------------------|---------------------------------|---------------------|---------------------------------|---------------------|
| | $\kappa = \bar{\kappa} = 0$ | | $\kappa = 10, \bar{\kappa} = 0$ | | $\kappa = 0, \bar{\kappa} = 10$ | |
| | Exact solution | Asymptotic solution | Exact solution | Asymptotic solution | Exact solution | Asymptotic solution |
| $c = b$ | | | | | | |
| 0.1 | 1.00127 | 1.00127 | 1.00202 | 1.00202 | 1.00127 | 1.00127 |
| 0.2 | 1.00995 | 1.00994 | 1.01604 | 1.01603 | 1.00995 | 1.00994 |
| 0.3 | 1.03231 | 1.03218 | 1.05357 | 1.05337 | 1.03229 | 1.03218 |
| 0.4 | 1.07273 | 1.07154 | 1.12634 | 1.12451 | 1.07252 | 1.07154 |
| 0.5 | 1.13357 | 1.12754 | 1.24931 | 1.23919 | 1.13241 | 1.12754 |
| 0.6 | 1.21601 | 1.19450 | 1.44757 | 1.40633 | 1.21129 | 1.19450 |
| 0.7 | 1.32168 | 1.26091 | 1.77371 | 1.63341 | 1.30567 | 1.26091 |
| 0.8 | 1.45572 | 1.31000 | 2.36346 | 1.92436 | 1.40693 | 1.31000 |
| 0.9 | 1.63650 | 1.32186 | 3.70965 | 2.27526 | 1.49059 | 1.32186 |
| 0.95 | 1.76495 | | 5.37187 | | 1.50131 | |
| 0.99 | 1.92430 | | 9.03787 | | 1.45262 | |
| 0.995 | 1.95550 | | 10.102 | | 1.43477 | |
| 0.999 | 1.9876 | | 11.40 | | 1.4130 | |
| $c = 3b$ | | | | | | |
| 0.1 | 1.00086 | | 1.00120 | | 1.00086 | |
| 0.2 | 1.00677 | | 1.00954 | | 1.00676 | |
| 0.3 | 1.02254 | | 1.03225 | | 1.02247 | |
| 0.4 | 1.05282 | | 1.07762 | | 1.05239 | |
| 0.5 | 1.10254 | | 1.15725 | | 1.10069 | |
| 0.6 | 1.17770 | | 1.29105 | | 1.17134 | |
| 0.7 | 1.28690 | | 1.51982 | | 1.26746 | |
| 0.8 | 1.44492 | | 1.94631 | | 1.38862 | |
| 0.9 | 1.68533 | | 2.93492 | | 1.51916 | |
| 0.95 | 1.86649 | | 4.15319 | | 1.56468 | |
| 0.99 | 2.08924 | | 6.82563 | | 1.54616 | |
| 0.995 | 2.13101 | | 7.60320 | | 1.53157 | |
| 0.999 | 2.1726 | | 8.56 | | 1.512 | |

not always enhance the net wall effect on the osmophoretic vesicle induced by the first plate only. This result reflects again the fact that the normal wall can affect the osmotic driving force and the hydrodynamic force on a vesicle in opposite directions as $\kappa \ll 1 + \bar{\kappa}$. Each force is increased in its own direction as the value of a/b turns small, but to a different degree, for the case of osmophoretic motion of a vesicle in a slit relative to that for the case of migration normal to a single plate. Thus, the net effect composed of these two opposite forces for the slit case is not necessarily to enhance that for the case of a single wall.

Fig. 4 shows the collocation results for the normalized velocity U/U_0 of a spherical vesicle undergoing osmophoresis perpendicular to two plane walls at various positions between them for a general case with $\kappa = 1 + \bar{\kappa}$ (U/U_0 is independent of the value of either κ or $\bar{\kappa}$ in this case). The dashed curves (with $a/b = \text{constant}$) illustrate the effect of the position of the second wall (at $z = c$) on the vesicle velocity for various values of the relative vesicle-to-first-wall spacing b/a . The solid curves (with $2a/(b+c) = \text{constant}$) indicate the variation of the vesicle velocity as a function of

the vesicle position at various values of the relative wall-to-wall spacing $(b+c)/2a$. As expected, the net wall effect for the given case is always to increase the osmophoretic mobility U/U_0 of the vesicle. At a constant value of $2a/(b+c)$, the vesicle has a smallest velocity when it is located midway between the two walls (with $c=b$). The osmophoretic velocity increases as the vesicle approaches either of the walls (or the ratio $b/(b+c)$ decreases). Interestingly, at some specified values of a/b for the osmophoretic vesicle near a first wall, the presence of a second plate is not necessarily to further increase the velocity of the vesicle, depending on the relative distance between the vesicle and the second plate.

Since the general problem of osmophoresis of a vesicle in an arbitrary direction between two parallel plane walls is linear, its solution can be obtained as the vectorial summation of the solutions for its two subproblems: motion perpendicular to the plane walls, which is examined in this paper, and motion parallel to the confining boundaries. The collocation solutions for the osmophoretic motion of a spherical vesicle parallel to two plane walls have already been obtained by Chen and Keh (2003). It was found that, when the walls

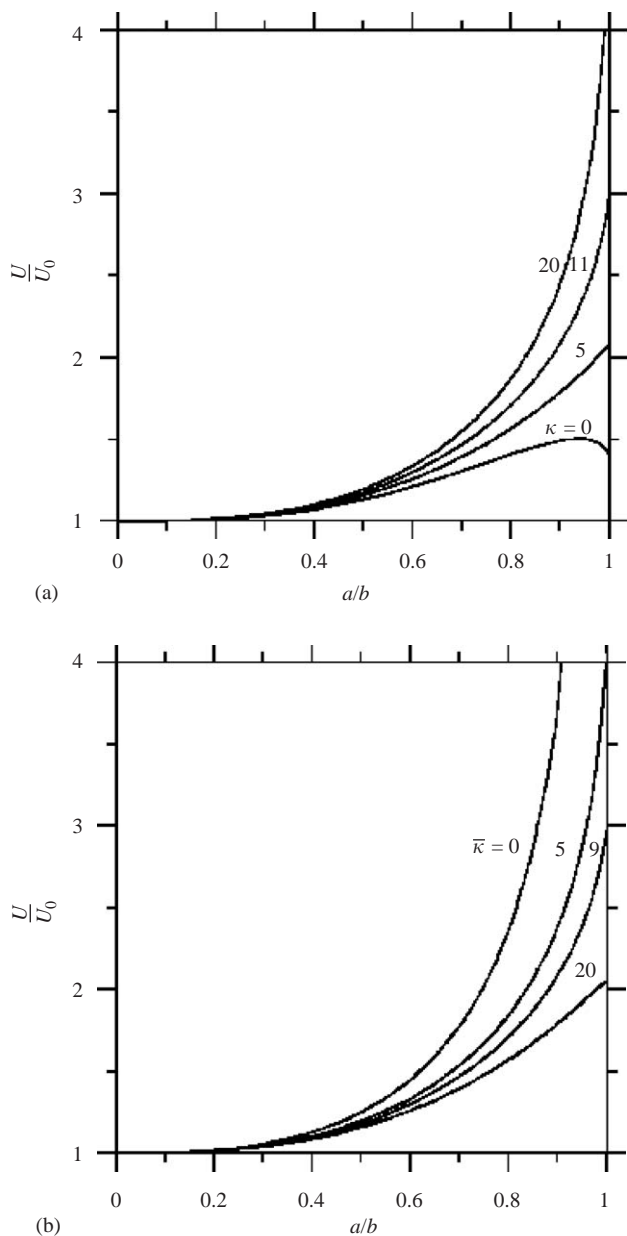


Fig. 3. Plots of the normalized mobility U/U_0 of a spherical vesicle situated midway between two parallel plane walls (with $c=b$) undergoing osmophoresis perpendicularly versus the separation parameter a/b : (a) for several values of κ with $\bar{\kappa}=10$; (b) for several values of $\bar{\kappa}$ with $\kappa=10$.

are prescribed with a linear concentration profile consistent with the far-field solute distribution, the wall-corrected normalized osmophoretic velocity of the vesicle also increases with an increase in the ratio $\kappa/(1+\bar{\kappa})$. A comparison between the Table 5 of Chen and Keh and our Table 4 shows that the plane walls exert the most influence on the vesicle when osmophoretic motion occurs normal to them, and the least in the case of osmophoresis parallel to them. Therefore, the direction of osmophoretic motion of a vesicle in the vicinity of two parallel plane walls is different from that of the solute concentration gradient, except when it is oriented parallel or perpendicular to the plane walls.

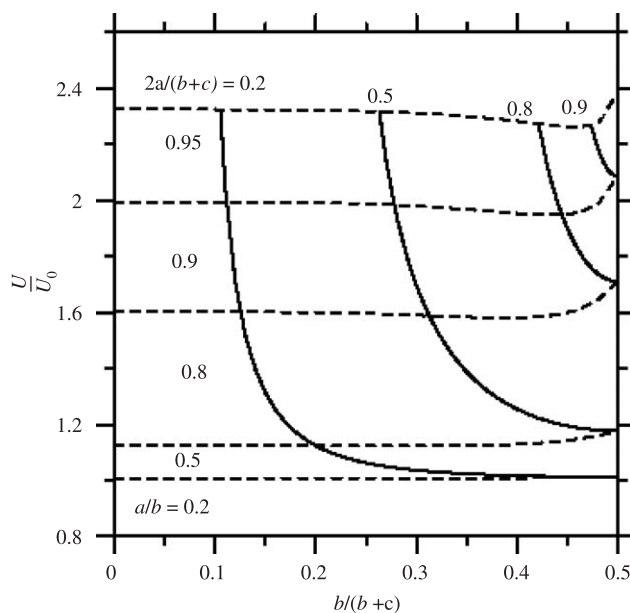


Fig. 4. Plots of the normalized osmophoretic velocity U/U_0 of a spherical vesicle perpendicular to two plane walls versus the ratio $b/(b+c)$ for the case of $\kappa = 1 + \bar{\kappa}$ with a/b and $2a/(b+c)$ as parameters.

4. Conclusions

The exact numerical solution and approximate analytical solution for the quasisteady osmophoretic motion of a spherical vesicle perpendicular to two plane walls at an arbitrary position between them have been obtained in this work by using the boundary-collocation technique and the method of reflections, respectively, in the limit of vanishingly small Peclet and Reynolds numbers. It has been found that the agreement between the collocation solution and the reflection solution is quite good, and the boundary effect on osmophoretic motion of vesicles is significant and complicated. The osmophoretic mobility of a vesicle in the proximity of plane walls is generally, but not necessarily, a monotonic increasing function of the separation parameter a/b . For the case of $\kappa \ll 1 + \bar{\kappa}$, the vesicle mobility may increase with an increase in a/b as a/b is small, and then decrease with an increase in a/b as a/b becomes large. This behavior reflects the competition between the hydrodynamic enhancement exerted by the neighboring walls on the vesicle migration and the possible osmotic retardation due to the solutal interaction between the vesicle and the walls.

The osmophoretic mobility of a spherical vesicle parallel to two infinite plane walls at an arbitrary position between them was calculated in a previous work (Chen and Keh, 2003) for various values of the parameters κ , $\bar{\kappa}$, a/b , and $b/(b+c)$. It was also found that, for the case of the confining walls prescribed with the far-field solute concentration profile under the situation of $\kappa \ll 1 + \bar{\kappa}$, the vesicle mobility first increases and then decreases with increasing a/b . When the gaps between the vesicle and the plane walls turn

thin, however, the vesicle can even migrate slower than it would as $a/b = 0$ (by as much as 8% for an example case of $\kappa = 0$, $\bar{\kappa} = 10$, $c = b$, and $a/b = 0.999$), which is not observed in our work for the osmophoresis normal to the plane walls. This difference between the boundary effects on osmophoresis of a vesicle near plane walls in parallel and perpendicular directions is interesting, suggesting that the effect of viscous interactions is stronger or the effect of solutal interactions is weaker in a transverse osmophoresis than in a parallel motion. In general, the net boundary effect on osmophoresis of a vesicle is stronger for the perpendicular migration. For the general problem of a vesicle undergoing osmophoresis in an arbitrary direction with respect to the two parallel plane walls, the solution can be obtained by adding both the parallel and transverse results vectorially.

Notation

| | |
|------------------------------|------------------------------------------------------------------------------------------------------------------|
| a | radius of the vesicle, m |
| A | osmophoretic mobility defined by Eq. (1b), $\text{m}^5 \text{s}^{-1}$ |
| b, c | the respective distances from the vesicle center to the two plates, m |
| B_n, D_n | coefficients in Eq. (22) or (23) for the flow field, $\text{m}^{n+2} \text{s}^{-1}$, $\text{m}^n \text{s}^{-1}$ |
| C | solute concentration field outside the vesicle, m^{-3} |
| C_0 | value of C_∞ at the position of vesicle center, m^{-3} |
| C_1 | solute concentration field inside the vesicle, m^{-3} |
| \bar{C} | average solute concentration inside the vesicle, m^{-3} |
| C_∞ | prescribed solute concentration field defined by Eq. (7), m^{-3} |
| $\mathbf{e}_r, \mathbf{e}_z$ | unit vectors |
| E_∞ | $= \nabla C_\infty $, m^{-4} |
| f^* | dimensionless Stokes resistance coefficient of the vesicle |
| F | hydrodynamic force exerted on the vesicle, N |
| F^* | normalized osmophoretic force on the vesicle defined by Eq. (27) |
| G | dimensionless parameter defined right after Eq. (A.4) |
| $G_n^{-1/2}$ | Gegenbauer polynomial of the first kind of order n and degree $-1/2$ |
| J_n | Bessel functions of the first kind of order n |
| L_p | hydraulic coefficient of the vesicle membrane, $\text{m}^2 \text{s kg}^{-1}$ |
| P_m | Legendre polynomial of order m |
| r | radial spherical coordinate, m |
| R | gas constant, J K^{-1} |
| R_m, \bar{R}_m | coefficients in Eqs. (10)–(12) for the solute concentration field, m^{m+2} , m^{-m+1} |

| | |
|---------------------|------------------------------------------------------------------------------------|
| T | absolute temperature, K |
| \mathbf{U}, U | osmophoretic velocity of the vesicle, m s^{-1} |
| \mathbf{U}_0, U_0 | osmophoretic velocity of an isolated vesicle defined by Eq. (1), m s^{-1} |
| \mathbf{v} | velocity field of the external fluid, m s^{-1} |
| v_ρ, v_z | components of \mathbf{v} in cylindrical coordinates, m s^{-1} |
| z | axial cylindrical coordinate, m |

Greek letters

| | |
|----------------------------------------|--------------------------------------------------------------------------------------------------|
| $\gamma_{1n}^{(j)}, \gamma_{2n}^{(j)}$ | functions of r and θ defined by Eqs. (B.5)–(B.8), m^{-n-1} , m^{-n+1} |
| $\delta_m^{(1)}, \delta_m^{(2)}$ | functions of r and θ defined by Eqs. (B.1)–(B.2), m^{-m-1} , m^{-m-2} |
| η | viscosity of the fluid, $\text{kg m}^{-1} \text{s}^{-1}$ |
| θ, ϕ | angular spherical coordinates |
| $\kappa, \bar{\kappa}$ | dimensionless parameters defined by Eq. (2) |
| λ | $= a/b$ |
| ρ | radial cylindrical coordinate, m |
| Ψ | Stokes stream function for the external fluid flow, $\text{m}^3 \text{s}^{-1}$ |

Subscripts

| | |
|-----|---------|
| p | vesicle |
| w | wall |

Acknowledgements

This research was partly supported by the National Science Council of the Republic of China.

Appendix A. Analysis of the osmophoresis of a spherical vesicle normal to one or two plane walls by a method of reflections

In this appendix, the quasisteady osmophoretic motion of a spherical vesicle perpendicular either to an infinite plane wall ($c \rightarrow \infty$) or to two parallel plane walls with equal distances from the vesicle ($c = b$), as shown in Fig. 1, will be analyzed using a method of reflections. The effect of the walls on the osmophoretic velocity \mathbf{U} of the vesicle is sought in expansions of λ , which equals a/b , the ratio of the vesicle radius to the distance between the vesicle center and the walls.

A.1. Motion normal to a plane wall

For the problem of osmophoretic motion of a spherical vesicle normal to an infinite plane wall, the governing equations (3a) and (14) must be solved by satisfying the boundary conditions (4)–(7) and (17)–(19) with $c \rightarrow \infty$. The

method-of-reflection solution consists of the following series, whose terms depend on increasing powers of λ :

$$C = C_0 - E_\infty z + C_p^{(1)} + C_w^{(1)} + C_p^{(2)} + C_w^{(2)} + \dots, \quad (\text{A.1a})$$

$$\mathbf{v} = \mathbf{v}_p^{(1)} + \mathbf{v}_w^{(1)} + \mathbf{v}_p^{(2)} + \mathbf{v}_w^{(2)} + \dots, \quad (\text{A.1b})$$

where subscripts w and p represent the reflections from wall and vesicle, respectively, and the superscript (i) denotes the i th reflection from that surface. In these series, all the expansion sets of the solute concentration and fluid velocity for the solution phase outside the vesicle must satisfy Eqs. (3a) and (14).

According to Eq. (A.1), the osmophoretic velocity of the vesicle can also be expressed in the series form:

$$\mathbf{U} = U_0 \mathbf{e}_z + \mathbf{U}^{(1)} + \mathbf{U}^{(2)} + \dots \quad (\text{A.2})$$

In this expression, $U_0 = AE_\infty$ is the osmophoretic velocity of an identical vesicle suspended freely in the unbounded solution phase given by Eq. (1); $\mathbf{U}^{(i)}$ is related to $C_w^{(i)}$ and $\mathbf{v}_w^{(i)}$ by a modified Faxen law (Keh and Tu, 2000):

$$\mathbf{U}^{(i)} = -A[\nabla C_w^{(i)}]_0 + [\mathbf{v}_w^{(i)}]_0 + \frac{a^2}{6}[\nabla^2 \mathbf{v}_w^{(i)}]_0, \quad (\text{A.3a})$$

where the subscript 0 to variables inside brackets denotes evaluation at the position of the vesicle center.

The solutions for the first reflected fields from the vesicle are

$$C_p^{(1)} = -GE_\infty a^3 r^{-2} \cos \theta, \quad (\text{A.4a})$$

$$\mathbf{v}_p^{(1)} = -U_0 a^3 r^{-3} (2 \cos \theta \mathbf{e}_r + \sin \theta \mathbf{e}_\theta), \quad (\text{A.4b})$$

where $G = (1 + \bar{\kappa} - \kappa)(2 + 2\bar{\kappa} + \kappa)^{-1}$. Obviously, $-1 \leq G \leq 1/2$, with the upper and lower bounds occurring at the limits $\kappa \ll 1 + \bar{\kappa}$ and $\kappa \gg 2(1 + \bar{\kappa})$, respectively. The velocity distribution shown in Eq. (A.4b) is identical to the irrotational flow surrounding an impermeable sphere moving with velocity $-2U_0 \mathbf{e}_z$.

The boundary conditions for the i th reflected fields from the wall are derived from Eqs. (6), (7), (18), and (19),

$$z = -b: C_w^{(i)} = -C_p^{(i)}, \quad (\text{A.5a})$$

$$\mathbf{v}_w^{(i)} = -\mathbf{v}_p^{(i)}; \quad (\text{A.5b})$$

$$r \rightarrow \infty, z \geq -b: C_w^{(i)} \rightarrow 0, \quad (\text{A.5c})$$

$$\mathbf{v}_w^{(i)} \rightarrow \mathbf{0}. \quad (\text{A.5d})$$

The solution of $C_w^{(1)}$ is obtained by applying Hankel transforms on the variable ρ in Eqs. (3a) and (A.5a,c) (taking $i = 1$), with the result

$$C_w^{(1)} = GE_\infty a^3 (2b + z)[(2b + z)^2 + \rho^2]^{-3/2}. \quad (\text{A.6a})$$

This reflected concentration field may be interpreted as arising from the reflection of the imposed field $E_\infty \mathbf{e}_z$ from a fictitious vesicle identical to the actual vesicle, its location being at the mirror-image position of the actual vesicle with respect to the plane $z = -b$ (i.e., at $x = 0, y = 0, z = -2b$). The solution for $\mathbf{v}_w^{(1)}$ can also be solved by applying Hankel transforms to the Stokes (14) twice and to boundary conditions (A.5b,d), which results in

$$\begin{aligned} \mathbf{v}_w^{(1)} = & 3U_0 a^3 \left\{ \rho(4b + 3z)[(2b + z)^2 + \rho^2]^{-5/2} \right. \\ & \left. - 10\rho(b + z)(2b + z)^2[(2b + z)^2 + \rho^2]^{-7/2} \right\} \mathbf{e}_\rho \\ & + U_0 a^3 \left\{ 2[(2b + z)^2 + \rho^2]^{-3/2} + 3[4(b + z) \right. \\ & \left. \times (2b + z) - \rho^2][(2b + z)^2 + \rho^2]^{-5/2} - 30\rho^2(b + z) \right. \\ & \left. \times (2b + z)[(2b + z)^2 + \rho^2]^{-7/2} \right\} \mathbf{e}_z. \quad (\text{A.6b}) \end{aligned}$$

The contributions of $C_w^{(1)}$ and $\mathbf{v}_w^{(1)}$ to the vesicle velocity are determined using Eq. (A.3),

$$\mathbf{U}_s^{(1)} = -A[\nabla C_w^{(1)}]_{r=0} = -\frac{1}{4}G\lambda^3 U_0 \mathbf{e}_z, \quad (\text{A.7a})$$

$$\mathbf{U}_h^{(1)} = \left[\mathbf{v}_w^{(1)} + \frac{a^2}{6} \nabla^2 \mathbf{v}_w^{(1)} \right]_{r=0} = \left(\lambda^3 - \frac{1}{2} \lambda^5 \right) U_0 \mathbf{e}_z, \quad (\text{A.7b})$$

$$\mathbf{U}^{(1)} = \mathbf{U}_s^{(1)} + \mathbf{U}_h^{(1)} = \left[\left(1 - \frac{1}{4}G \right) \lambda^3 - \frac{1}{2} \lambda^5 \right] U_0 \mathbf{e}_z. \quad (\text{A.7c})$$

Eq. (A.7a) shows that the reflected solute concentration field from the plane wall can decrease (if $G > 0$ or $\kappa < 1 + \bar{\kappa}$) or increase (if $G < 0$ or $\kappa > 1 + \bar{\kappa}$) the osmophoretic velocity of the vesicle, while Eq. (A.7b) indicates that the reflected velocity field is to increase this velocity; the net effect of the reflected fields is expressed by Eq. (A.7c), which enhances the movement of the vesicle, no matter what the values of G (or κ and $\bar{\kappa}$) and λ are. When $G = 0$ (or $\kappa = 1 + \bar{\kappa}$), the reflected concentration field makes no contribution to the osmophoretic velocity.

The solution for the second reflected fields from the vesicle is

$$\begin{aligned} C_p^{(2)} = & E_\infty \left[\frac{1}{4}G^2 \lambda^3 a^3 r^{-2} \cos \theta + \frac{3}{16}GH\lambda^4 a^4 r^{-3} \right. \\ & \left. \times (3 \cos^2 \theta - 1) + O(\lambda^5 a^5) \right], \quad (\text{A.8a}) \end{aligned}$$

$$\begin{aligned} \mathbf{v}_p^{(2)} = & U_0 \left[\frac{1}{4}G\lambda^3 a^3 r^{-3} (2 \cos \theta \mathbf{e}_r + \sin \theta \mathbf{e}_\theta) \right. \\ & \left. + \frac{3}{32}(2GW + 15)\lambda^4 a^2 r^{-2} (3 \cos^2 \theta - 1) \mathbf{e}_r \right. \\ & \left. + O(\lambda^4 a^4, \lambda^5 a^3) \right], \quad (\text{A.8b}) \end{aligned}$$

where $H = (2 + \bar{\kappa} - \kappa)(6 + 3\bar{\kappa} + 2\kappa)^{-1}$ and $W = 5(2 + 2\bar{\kappa} + \kappa)(6 + 3\bar{\kappa} + 2\kappa)^{-1}$.

The boundary conditions for the second reflected fields from the wall are obtained by substituting the results of $C_p^{(2)}$ and $\mathbf{v}_p^{(2)}$ into Eq. (A.5), with which Eqs. (3a) and (14) can be solved as before to yield

$$[\nabla C_w^{(2)}]_{r=0} = E_\infty [-\frac{1}{16}G^2\lambda^6 + O(\lambda^9)]\mathbf{e}_z, \quad (\text{A.9a})$$

$$\left[\mathbf{v}_w^{(2)} + \frac{a^2}{6}\nabla^2\mathbf{v}_w^{(2)} \right]_{r=0} = U_0 \left\{ \frac{1}{128}[135 - 2(16 + 9W)G]\lambda^6 + \frac{1}{8}\left[G + \frac{3}{64}(2GW - 15)\right]\lambda^8 + O(\lambda^9) \right\} \mathbf{e}_z. \quad (\text{A.9b})$$

The contribution of the second reflected fields to the vesicle velocity is obtained by combining Eqs. (A.3) and (A.9), which gives

$$\mathbf{U}^{(2)} = U_0 \left\{ \frac{1}{128}[135 - 2(16 + 9W)G + 8G^2]\lambda^6 + \frac{1}{8}\left[G + \frac{3}{64}(2GW - 15)\right]\lambda^8 + O(\lambda^9) \right\} \mathbf{e}_z. \quad (\text{A.10})$$

Obviously, $\mathbf{U}^{(3)}$ will be $O(\lambda^9)$. With the substitution of Eqs. (A.7c) and (A.10) into Eq. (A.2), the osmophoretic velocity of the vesicle can be expressed as $\mathbf{U} = U\mathbf{e}_z$ with

$$U = U_0 \left\{ 1 + (1 - \frac{1}{4}G)\lambda^3 - \frac{1}{2}\lambda^5 + \frac{1}{128}[135 - 2(16 + 9W)G + 8G^2]\lambda^6 + \frac{1}{8}\left[G + \frac{3}{64}(2GW - 15)\right]\lambda^8 + O(\lambda^9) \right\}. \quad (\text{A.11})$$

Owing to the linearity of the problem, the above analysis is valid when the vesicle is either approaching the plane wall or receding from it.

A.2. Motion normal to two parallel plane walls

For the problem of osmophoretic motion of a spherical vesicle perpendicular to two infinite plane walls with equal distances from the vesicle, the boundary conditions corresponding to governing equations (3a) and (14) are given by Eqs. (4)–(7) and (17)–(19) with $c = b$. With $\lambda = a/b \ll 1$, the series expansions of the solute concentration, fluid velocity, and vesicle velocity given by Eqs. (A.1), (A.2), and (A.4) remain valid here. From Eqs. (5)–(7), (18), and (19), the boundary conditions for $C_w^{(i)}$ and $\mathbf{v}_w^{(i)}$ are found to be

$$|z| = b: C_w^{(i)} = -C_p^{(i)}, \quad (\text{A.12a})$$

$$\mathbf{v}_w^{(i)} = -\mathbf{v}_p^{(i)}; \quad (\text{A.12b})$$

$$\rho \rightarrow \infty: C_w^{(i)} \rightarrow 0, \quad (\text{A.12c})$$

$$\mathbf{v}_w^{(i)} \rightarrow \mathbf{0}. \quad (\text{A.12d})$$

The first wall-reflected fields can be solved by the same method as used for the case of a single plane wall in the

previous subsection, with the result

$$C_w^{(1)} = GE_\infty a \lambda^2 \int_0^\infty \frac{1 + e^{-2\alpha}}{\sinh(2\alpha)} \alpha \cosh\left(\frac{\alpha}{b}z\right) J_0\left(\frac{\alpha}{b}\rho\right) d\alpha, \quad (\text{A.13a})$$

$$\mathbf{v}_w^{(1)} = U_0 \lambda^3 \int_0^\infty \alpha^2 \left[E(\alpha, z) J_1\left(\frac{\alpha}{b}\rho\right) \mathbf{e}_\rho + F(\alpha, z) J_0\left(\frac{\alpha}{b}\rho\right) \mathbf{e}_z \right] d\alpha, \quad (\text{A.13b})$$

where

$$E(\alpha, z) = \frac{2}{2\alpha + \sinh(2\alpha)} \left[(1 - \alpha - e^{-\alpha} \sinh \alpha) \times \sinh\left(\frac{\alpha}{b}z\right) + \frac{\alpha}{b}z \cosh\left(\frac{\alpha}{b}z\right) \right], \quad (\text{A.14a})$$

$$F(\alpha, z) = \frac{2}{2\alpha + \sinh(2\alpha)} \left[(\alpha + e^{-\alpha} \sinh \alpha) \times \cosh\left(\frac{\alpha}{b}z\right) - \frac{\alpha}{b}z \sinh\left(\frac{\alpha}{b}z\right) \right]. \quad (\text{A.14b})$$

The contributions of $C_w^{(1)}$ and $\mathbf{v}_w^{(1)}$ to the vesicle velocity are determined using Eq. (A.3), which lead to a result similar to Eq. (A.7),

$$\mathbf{U}_s^{(1)} = -A[\nabla C_w^{(1)}]_{r=0} = d_1 G \lambda^3 U_0 \mathbf{e}_z, \quad (\text{A.15a})$$

$$\mathbf{U}_h^{(1)} = \left[\mathbf{v}_w^{(1)} + \frac{a^2}{6}\nabla^2\mathbf{v}_w^{(1)} \right]_{r=0} = (d_2 \lambda^3 + d_3 \lambda^5) U_0 \mathbf{e}_z, \quad (\text{A.15b})$$

$$\mathbf{U}^{(1)} = \mathbf{U}_s^{(1)} + \mathbf{U}_h^{(1)} = [(d_2 + d_1 G)\lambda^3 + d_3 \lambda^5] U_0 \mathbf{e}_z, \quad (\text{A.15c})$$

where

$$d_1 = - \int_0^\infty \frac{1 + e^{-2\alpha}}{\sinh(2\alpha)} \alpha^2 d\alpha = -0.60103, \quad (\text{A.16a})$$

$$d_2 = 2 \int_0^\infty \frac{\sinh(\alpha)e^{-\alpha} + \alpha}{2\alpha + \sinh(2\alpha)} \alpha^2 d\alpha = 1.58153, \quad (\text{A.16b})$$

$$d_3 = -\frac{2}{3} \int_0^\infty \frac{\alpha^4}{2\alpha + \sinh(2\alpha)} d\alpha = -0.88351. \quad (\text{A.16b})$$

Again, Eq. (A.15a) shows that the reflected concentration field from the confining walls can decrease (if $G > 0$ or $\kappa < 1 + \bar{\kappa}$) or increase (if $G < 0$ or $\kappa > 1 + \bar{\kappa}$) the vesicle velocity, while Eq. (A.15b) indicates that the reflected velocity field is to increase this velocity; the net effect is expressed by Eq. (A.15c), which always enhances the movement of the vesicle.

Analogous to the previous case, the results of the second reflections can be obtained as

$$C_p^{(2)} = -E_\infty [d_1 G^2 \lambda^3 a^3 r^{-2} \cos \theta + O(\lambda^5 a^5)], \quad (\text{A.17a})$$

$$\mathbf{v}_p^{(2)} = -U_0 d_1 G \lambda^3 a^3 r^{-3} (2 \cos \theta \mathbf{e}_r + \sin \theta \mathbf{e}_\theta) + O(\lambda^5 a^3), \quad (\text{A.17b})$$

$$[\nabla C_w^{(2)}]_{r=0} = -E_\infty [d_1^2 G^2 \lambda^6 + O(\lambda^9)] \mathbf{e}_z, \quad (\text{A.18a})$$

$$\left[\mathbf{v}_w^{(2)} + \frac{a^2}{6} \nabla^2 \mathbf{v}_w^{(2)} \right]_{r=0} = U_0 [d_1 d_2 G \lambda^6 + d_1 d_3 G \lambda^8 + O(\lambda^9)] \mathbf{e}_z, \quad (\text{A.18b})$$

and

$$\mathbf{U}^{(2)} = U_0 [(d_1^2 G^2 + d_1 d_2 G) \lambda^6 + d_1 d_3 G \lambda^8 + O(\lambda^9)] \mathbf{e}_z. \quad (\text{A.19})$$

Note that the $\lambda^4 a^2$ and $\lambda^4 a^4$ terms in the expressions for $C_p^{(2)}$ and $\mathbf{v}_p^{(2)}$ vanish.

With the combination of Eqs. (A.2), (A.15c), and (A.19), the vesicle velocity can be expressed as $\mathbf{U} = U_0 \mathbf{e}_z$ with

$$U = U_0 [1 + (d_2 + d_1 G) \lambda^3 + d_3 \lambda^5 + (d_1^2 G^2 + d_1 d_2 G) \lambda^6 + d_1 d_3 G \lambda^8 + O(\lambda^9)]. \quad (\text{A.20})$$

This result is valid for a vesicle undergoing osmophoresis toward either of the two plane walls.

Appendix B. Definitions of some functions in Section 2

The functions $\delta_m^{(1)}$ and $\delta_m^{(2)}$ in Eqs. (12) and (13) are defined by

$$\delta_m^{(1)}(r, \theta) = \int_0^\infty [S'_m(\omega) e^{\omega r \cos \theta} + S''_m(\omega) e^{-\omega r \cos \theta}] \times \omega J_0(\omega r \sin \theta) d\omega + r^{-m-1} P_m(\cos \theta), \quad (\text{B.1})$$

$$\delta_m^{(2)}(r, \theta) = \int_0^\infty \omega^2 \{ [S'_m(\omega) e^{\omega r \cos \theta} - S''_m(\omega) e^{-\omega r \cos \theta}] \times J_0(\omega r \sin \theta) \cos \theta - [S'_m(\omega) e^{\omega r \cos \theta} + S''_m(\omega) e^{-\omega r \cos \theta}] J_1(\omega r \sin \theta) \sin \theta \} d\omega - (m+1) r^{-m-2} P_m(\cos \theta), \quad (\text{B.2})$$

where

$$S'_m(\omega) = -\frac{\omega^{m-1}}{m!} \frac{[1 - (-1)^m e^{-2b\omega}]}{[e^{2c\omega} - e^{-2b\omega}]}, \quad (\text{B.3})$$

$$S''_m(\omega) = -\frac{\omega^{m-1}}{m!} \frac{[(-1)^m - e^{-2c\omega}]}{[e^{2b\omega} - e^{-2c\omega}]}. \quad (\text{B.4})$$

The functions $\gamma_{in}^{(j)}$ for i and j equal to 1 or 2 in Eqs. (23) and (24) are defined by

$$\gamma_{in}^{(1)}(r, \theta) = \int_0^\infty [G'_+(\sigma, \eta) B'_{in}(\omega, -b) - G''_+(\eta, \sigma) B'_{in}(\omega, c) - G'_+(\sigma, \eta) B''_{in}(\omega, -b) + G''_+(\eta, \sigma) B''_{in}(\omega, c)] \times \omega J_1(\omega r \sin \theta) d\omega + r^{-n+2i-3} [(n+1) G_{n+1}^{-1/2} \times (\cos \theta) \csc \theta - 2(i-1) G_n^{-1/2} (\cos \theta) \cot \theta], \quad (\text{B.5})$$

$$\gamma_{in}^{(2)}(r, \theta) = \int_0^\infty [-G'_-(\sigma, \eta) B'_{in}(\omega, -b) + G'_-(\eta, \sigma) B'_{in}(\omega, c) + G''_-(\sigma, \eta) B''_{in}(\omega, -b) - G''_-(\eta, \sigma) B''_{in}(\omega, c)] \times \omega J_0(\omega r \sin \theta) d\omega + r^{-n+2i-3} [P_n(\cos \theta) + 2(i-1) G_n^{-1/2} (\cos \theta)], \quad (\text{B.6})$$

where

$$B'_{1n}(\omega, z) = -\frac{1}{n!} \left(\frac{\omega |z|}{z} \right)^{n-1} e^{-\omega |z|}, \quad (\text{B.7})$$

$$B''_{1n}(\omega, z) = -\frac{\omega^{n-1}}{n!} \left(\frac{|z|}{z} \right)^n e^{-\omega |z|}, \quad (\text{B.8})$$

$$B'_{2n}(\omega, z) = -\frac{1}{n!} \left(\frac{\omega |z|}{z} \right)^{n-3} \times [(2n-3)\omega |z| - n(n-2)] e^{-\omega |z|}, \quad (\text{B.9})$$

$$B''_{2n}(\omega, z) = -\frac{\omega^{n-3}}{n!} \left(\frac{|z|}{z} \right)^n [(2n-3)\omega |z| - (n-1)(n-3)] e^{-\omega |z|}, \quad (\text{B.10})$$

$$G'_\pm(\mu, \nu) = \tau \mu \nu \left(\frac{\sinh \mu}{\mu} \pm \frac{\sinh \tau \sinh \nu}{\tau \nu} \right) \times (\sinh^2 \tau - \tau^2)^{-1}, \quad (\text{B.11})$$

$$G''_\pm(\mu, \nu) = \tau \left[\nu \left(\cosh \mu - \frac{\sinh \tau \sinh \nu}{\tau \nu} \right) \pm \mu \left(\frac{\sinh \mu}{\mu} - \frac{\sinh \tau \cosh \nu}{\tau} \right) \right] \times (\sinh^2 \tau - \tau^2)^{-1}, \quad (\text{B.12})$$

$$\sigma = \omega(r \cos \theta + b), \quad \eta = \omega(r \cos \theta - c), \quad \tau = \omega(b + c). \quad (\text{B.13})$$

References

- Anderson, J.L., 1983. Movement of a semipermeable vesicle through an osmotic gradient. *Physics of Fluids* 26, 2871–2879.
- Anderson, J.L., 1984. Shape and permeability effects on osmophoresis. *PhysicoChemical Hydrodynamics* 5, 205–216.
- Anderson, J.L., 1986. Transport mechanisms of biological colloids. *Annals of the New York Academy of Sciences (Biochemical Engineering IV)* 469, 166–177.
- Berg, H.C., Turner, L., 1990. Chemotaxis of bacteria in glass capillary arrays. *Biophysics Journal* 58, 919–930.
- Brenner, H., 1961. The slow motion of a sphere through a viscous fluid towards a plane surface. *Chemical Engineering Science* 16, 242–251.
- Chen, P.Y., Keh, H.J., 2003. Boundary effects on osmophoresis: motion of a spherical vesicle parallel to two plane walls. *Chemical Engineering Science* 58, 4449–4464.
- Ganatos, P., Weinbaum, S., Pfeffer, R., 1980. A strong interaction theory for the creeping motion of a sphere between plane parallel boundaries. Part 1. Perpendicular motion. *Journal of Fluid Mechanics* 99, 739–753.
- Gordon, L.G.M., 1981. Osmophoresis. *Journal of Physical Chemistry* 85, 1753–1755.
- Happel, J., Brenner, H., 1983. *Low Reynolds Number Hydrodynamics*. Nijhoff, Dordrecht, The Netherlands.

- Keh, H.J., Tu, H.J., 2000. Osmophoresis in a dilute suspension of spherical vesicles. *International Journal of Multiphase Flow* 26, 125–145.
- Keh, H.J., Yang, F.R., 1993a. Boundary effects on osmophoresis: motion of a vesicle normal to a plane wall. *Chemical Engineering Science* 48, 609–616.
- Keh, H.J., Yang, F.R., 1993b. Boundary effects on osmophoresis: motion of a vesicle in an arbitrary direction with respect to a plane wall. *Chemical Engineering Science* 48, 3555–3563.
- Maude, A.D., 1961. End effects in a falling-sphere viscometer. *British Journal of Applied Physics* 12, 293–295.
- Nardi, J., Bruinsma, R., Sackmann, E., 1999. Vesicles as osmotic motors. *Physics Review Letters* 82, 5168–5171.
- O'Brien, V., 1968. Form factors for deformed spheroids in Stokes flow. *A.I.Ch.E. Journal* 14, 870–875.
- Pope, C.G., 1982. Investigation of osmophoresis. *Journal of Physical Chemistry* 86, 1869–1870.
- Zinemanas, D., Nir, A., 1995. Osmophoretic motion of deformable particles. *International Journal of Multiphase Flow* 21, 787–800.